# TRACKING THE EVOLUTION OF LUMINOUS RED GALAXIES USING THE DARK ENERGY SURVEY

An Undergraduate Research Scholars Thesis

by

NICHOLAS PAYNE MONDRIK

Submitted to Honors and Undergraduate Research
Texas A&M University
in partial fulfillment of the requirements for the designation as

UNDERGRADUATE RESEARCH SCHOLAR

Approved by
Research Advisor: Casey Papovich

May 2015

Major: Physics

# TABLE OF CONTENTS

Page

ABSTRACT . . . . . 1

DEDICATION . . . . . 2

ACKNOWLEDGMENTS . . . . . 3

CHAPTER

I INTRODUCTION . . . . . 4

Early-type galaxies and their stellar populations . . . . . 4

Data and methods . . . . . 8

II DATA . . . . . 15

FAST parameters and data reduction . . . . . 15

III DISCUSSION . . . . . 24

Mass evolution . . . . . 24

Future work . . . . . 28

REFERENCES . . . . . 30

# ABSTRACT

Tracking the Evolution of Luminous Red Galaxies
Using the Dark Energy Survey. (May 2015)

Nicholas Payne Mondrik
Department of Physics & Astronomy
Texas A&M University

Research Advisor: Dr. Casey Papovich
Department of Physics

Galaxies form the fundamental building blocks of the large scale structure of the universe. As such, understanding their formation and evolution plays a key role in determining how our universe evolved to its present state. We present in this thesis an analysis of the mass and color evolution (from $z = 0.1$ to $z = 1$) of a subset of galaxies called luminous red galaxies (LRGs) taken from the Dark Energy Survey. LRGs are the most massive galaxies found in the nearby universe, and typically reside in galaxy clusters. Their red colors indicate that they are dominated by old stellar populations, with most forming just a few billion years after the big bang. Data from the Dark Energy Survey allows us to sample the growth of LRGs in a large portion of the sky (5000 sq. deg.) over half the lifetime of the universe. We find that most LRGs in our sample have a mass between $10^{10}$ and $10^{11}$ solar masses. We also find that the color evolution is well modeled by a simple stellar population with a formation redshift of between z = 5 and z = 3, except in the $g - r$ color. We also explore the differences between observed and theoretical evolutionary models, which could be caused by model deficiencies or progenitor bias in our galaxy sampling.

# DEDICATION

For my parents, Don & Milissa, and their unwavering support of all my endeavors.

# ACKNOWLEDGMENTS

I would like to thank Dr. Jennifer Marshall and Dr. Darren DePoy for helping foster my love of astronomy. The amount of help and support they've given me over the past couple of years in learning astronomy is more than I could have ever imagined.

I would also like to thank Dr. Papovich, who is also responsible (in no small part) for showing me how exciting astronomy really is. Dr. Papovich's enthusiasm for astronomy is infectious, and his ability to communicate his passion to others will serve our department well for years to come.

# CHAPTER I

# INTRODUCTION

## Early-type galaxies and their stellar populations

### *Morphology*

Morphology has been the driving force behind the classification of galaxies since the days of Edwin Hubble. Hubble originally sorted galaxies into two main groups: elliptical galaxies (also called early-type galaxies, or ETGs), and spiral galaxies (also known as late-type galaxies, or LTGs). A third class, called irregulars, forms the catchall for galaxies which do not fit into the previous two. Spiral galaxies are further sorted according to the presence of a bar of stars in the central bulge of the galaxies, with those possessing a bar referred to as barred spirals. Morphology however, is a mutable property, and in order to understand how ETGs and LTGs formed, we must understand the physical processes that drive the formation, growth, and composition of these galaxies. In this thesis, we focus on the growth of a sub-type of ETGs known as luminous red galaxies (LRGs), which are a relatively homogeneous population of ETGs [Postman and Lauer, 1995] typically residing in galaxy clusters. LRGs are some of the most massive galaxies in the nearby universe, and measuring their growth and evolution allows us to test theories of stellar population evolution, cosmological dark matter dynamics, as well as theories of galaxy formation and assembly. Figure I.1 shows typical examples of the shape and color of LRGs.


Fig. I.1. Examples of Luminous Red Galaxies (LRGs) from the Sloan Digital Sky Survey (http://www.sdss.org/).

*Formation and characteristics of early-type galaxies*

Early-type galaxies are separated into sub-classes by their degree of ellipticity, with E0 ETGs being nearly spherical, and E7 galaxies being almost flat and highly eccentric. When Hubble first proposed his theory of galaxy evolution, he posited that galaxies form as E0 galaxies and evolve into spiral galaxies, following what is now known as the Hubble Tuning Fork, shown in figure I.2. Astronomers now know however, that evolution likely occurs in the opposite direction, with blue spiral galaxies forming in host dark matter halos and evolving into elliptical galaxies.

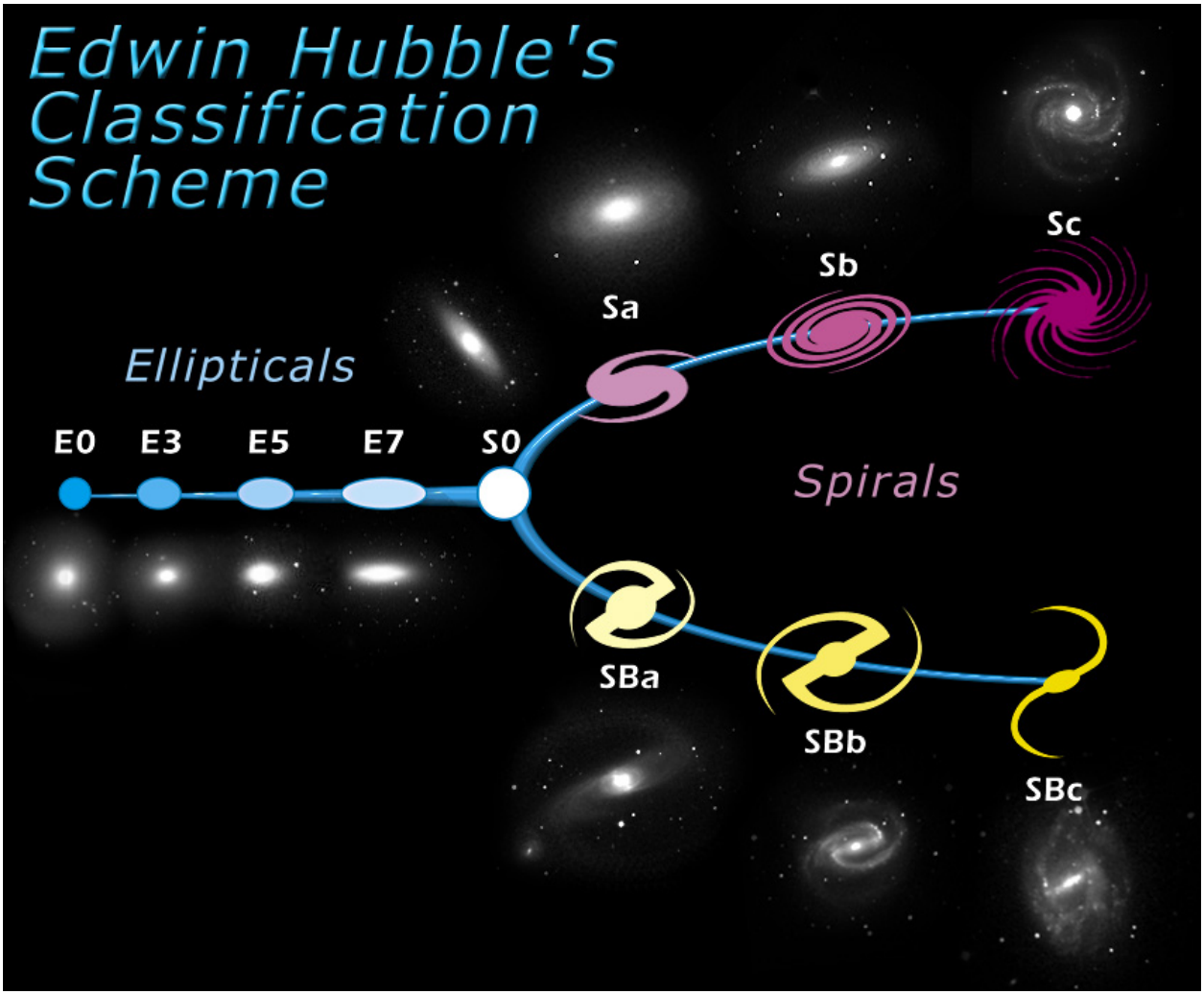


Fig. I.2. The Hubble Tuning Fork diagram (from the Space Telescope Science Institute http://www.stsci.edu/portal/).

The first major attempt to explain galaxy formation and evolution was the Eggen, Lynden-Bell, and Sandage (ELS) model [Eggen et al., 1962]. In the ELS model (also known as the monolithic collapse model), spiral galaxies form from the gravitational collapse of a large cloud of gas to form a disk. The stars formed from this gravitational collapse should follow highly eccentric, plunging orbits, with no net rotation among stars in the galaxy. The next step in galaxy evolution was made by Searle and Zinn [Searle and Zinn, 1978], who extended the ELS model by allowing proto-galaxies to form, then merge into a host galaxy. The SZ model was an improvement over the ELS model in that it provided a better explanation for irregularities in the population of the Milky Way's stellar halo. The modern interpretation of galaxy formation is very similar to the SZ model in that many galaxies form early in the universe and merge and grow into galaxies we observe today. An important distinction between the SZ model and the modern theory is that the major gravitational component that dominates the evolution of the proto-galaxies is not visible matter, but rather the host dark matter halos of the proto-galaxies.

Spiral galaxies form inside dark matter halos from the gravitational collapse of gas clouds, forming a disk shape due to the initial angular momentum of the gas cloud. These young galaxies are characterized by their very blue colors, due to the high amount of star formation occurring in the galaxies. Once these galaxies begin to run out of gas from which new stars are formed, their colors become redder as the short-lived, blue stars die out and are not replaced. This leads galaxies to become redder as they age, but does not account for the change in shape between spiral galaxies and ETGs. This change in morphology is thought to be due to mergers between host dark matter halos (and, by extension, the galaxies within them). As the blue spiral galaxies merge, their disk shape is disrupted by the collision, which, over the course of many major and minor mergers, produces elliptical galaxies. Thus, this process of hierarchical merging combined with stellar evolution models [Bruzual and Charlot, 2003], allows us to describe ETGs quantitatively as systems of old, red stars with large velocity dispersions and little to no star formation.

*Growth of ETGs since $z \approx 1$*

Modern studies [Toft et al., 2007, van Dokkum et al., 2010] show that ETGs were still forming stars until $z \approx 2$, when the universe was about 3 Gy old. Since $z \approx 2$, ETGs have been shown to grow around a relatively compact core [van Dokkum et al., 2010] almost entirely via mergers and accretion events. This model of growth via merging and accretion has not, however, been tested for large numbers of high-mass ETGs (of which LRGs are a subset), an issue this thesis attempts to address.

*Goals of this work*

To quantify the growth of these LRGs, we use two main techniques: cumulative number density comparisons [Behroozi et al., 2013] and spectral energy density (SED) fitting via FAST [Kriek et al., 2009]. We track the mass evolution of LRGs as predicted by using Behroozi et al. [2013], Muzzin et al. [2013], and Bell et al. [2003] and compare theoretical predictions of galaxy mass evolution to observational data fit using FAST. We also compare the color evolution of selected progenitor galaxies using the population modeling code EzGal (http://www.baryons.org/EzGal/) with population models from Conroy et al. [2009] and Conroy and Gunn [2010].

**Data and methods**

*The Dark Energy Survey*

The Dark Energy Survey [The Dark Energy Survey Collaboration, 2005] is a project currently underway on the Blanco 4-m telescope at Cerro Tololo Inter-American Observatory in Chile. Using a modern wide-field CCD, the DES will image approximately 5000 sq. deg. of southern sky down to roughly 24th magnitude over 5 years. Note that the sky itself is not back - typical sky

background is around 19th-20th magnitude [Krisciunas, 1997]. This means the DES will find stars darker than the sky. The goal of DES is to measure dark energy and dark matter densities in order to constrain the dark energy equation of state. To do this, DES will employ four main techniques: galaxy clustering measurements, weak lensing tomography, galaxy angular clustering, and supernova luminosity distances. DES will have a photometric precision of $\leq 2\%$, which is required to obtain accurate photometric redshifts for the weak lensing, angular clustering, and supernova distance measurements. The accurate photometric redshifts allow for precise measurements of the mass evolution across cosmic time via number density matching. The accuracy of the photometry also allows for very precise SED fitting, which ensures the accuracy of parameters such as stellar mass and star formation rates.

*Redmapper*

For our observational data, we employ the Redmapper [Rykoff et al., 2014] DES catalog. The Redmapper DES catalog [E. Rykoff - private communication] is an LRG catalog containing photometry (images taken though different bandpasses in wavelength) and photometric redshifts ($0 < z < 1$) of galaxies taken from the Dark Energy Survey (DES, The Dark Energy Survey Collaboration 2005). Photometric redshifts for LRGs are possible to derive via photometry due to the homogeneity of the LRG population. Redmapper leverages the fact that LRGs appear to have a common formation epoch, and that we understand how their stellar populations evolve afterwards. This process of coevolution leads to a very small dispersion in color for the LRG population. By searching for galaxies whose colors fall within a specific range, Redmapper can efficiently select LRGs from a larger galaxy sample. Figures I.3 and I.4 show examples of this homogeneity in both a quantitative and qualitative sense.

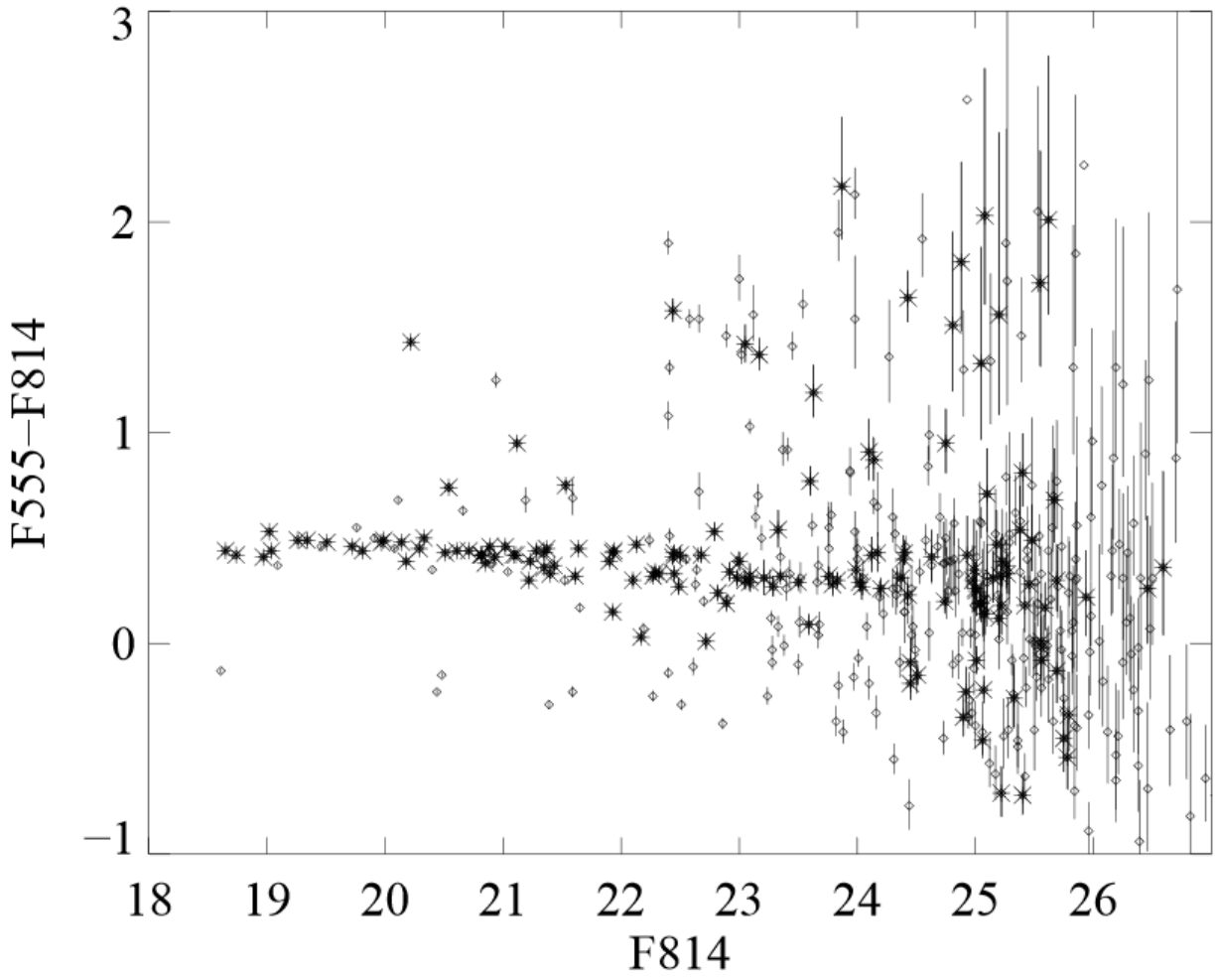


Fig. I.3. A color-magnitude diagram of the Abell 2390 galaxy cluster. Tight dispersion along the vertical axis is indicative of a homogeneous population. The scatter along the horizontal axis reflects the differing intrinsic luminosities of the cluster members. (Figure from Gladders and Yee 2000).

Fig. I.4. A Hubble Space Telescope image of the Abell 1689 galaxy cluster. LRGs and other ETGs are the elliptical or spheroidal reddish galaxies. Note that all ETGs and LRGs appear fairly similar in overall color. (Image from http://www.spacetelescope.org).

*Cumulative number density*

In order to track the mass evolution of LRGs, some method of comparing galaxies across cosmic timescales is required. Our chosen method employs cumulative number densities to measure how the masses of galaxies evolve as a function of time or redshift. However, accurate mass functions are required to convert number densities into stellar masses. For this thesis, we employ the stellar mass functions of Bell et al. [2003] (at $z = 0.1$) and Muzzin et al. [2013] (for $z > 0.1$) and number density calculations from Behroozi et al. [2013]. The number density calculations of Behroozi et al. [2013] make use of cosmological dark matter simulations which allow us to determine the effects of mergers on the mass history of dark matter halos, and therefore galaxies. This is in contrast with the typical practice of assuming a constant number density in time, and can have a significant effect of the predicted masses of progenitor galaxies, as shown in figure I.5. Figure I.5(b) clearly shows why this effect should be taken into account. For a galaxy with a mass of $\sim 10^{11.5}$ at $z = 0.35$, there is a difference of almost 0.2 dex (a factor of 1.6) in predicted progenitor mass. By accounting for mergers, the mass of progenitors is decreased, since the galaxies are allowed to grow not only by forming new stars (which slows rapidly after $z \approx 2$), but also by accreting mass in the form of smaller galaxies.

*Spectral energy density*

Spectral energy density (SED) is the amount of energy per unit wavelength emitted by a source. The blue end of a galaxy's SED is dominated by the hot,high-mass, blue stars. The red end on the other hand, reflects the lower-mass stellar population. Because the mass to light ratio of these two populations is very different, the shape of the SED (measured here by its photometric proxy, color) can be used to derive the overall mass to light ratio of the galaxy. Since we have estimated the redshift to the galaxy, we can use a cosmological distance estimate to derive the total luminosity of the galaxy, and hence, its mass. This conversion is done via an IDL code known as FAST [Kriek et al., 2009]. SED fitting is done by assuming certain parameters about the galaxy in question

(redshift, metallicity, star formation history, etc.) and then generating templates and matching the template SEDs to photometry of the galaxy. Since photometry provides only one point per band to fit to an SED, it is imperative that the photometry be as accurate as possible in order to select the best template. Once the best template is located, the galaxy is assumed to have parameters matching the generated SED, which allows for acquisition of quantities such as stellar mass and star formation rates that are not directly available from the raw data. There do, however, exist limitations on SED fitting. Without access to supercomputing facilities, models must make many assumptions, especially with regard to dust and metallicity of the galaxy to be fit. In addition to the assumptions made by FAST, the limitation on number of photometric bands to be fit can cause improper SEDs to be selected as best fit SEDs. In both of these cases however, large numbers come to our aid. With over 500,000 galaxies to be fit, catastrophic outliers tend to be overwhelmed by the bulk of the data, and so are not an issue.

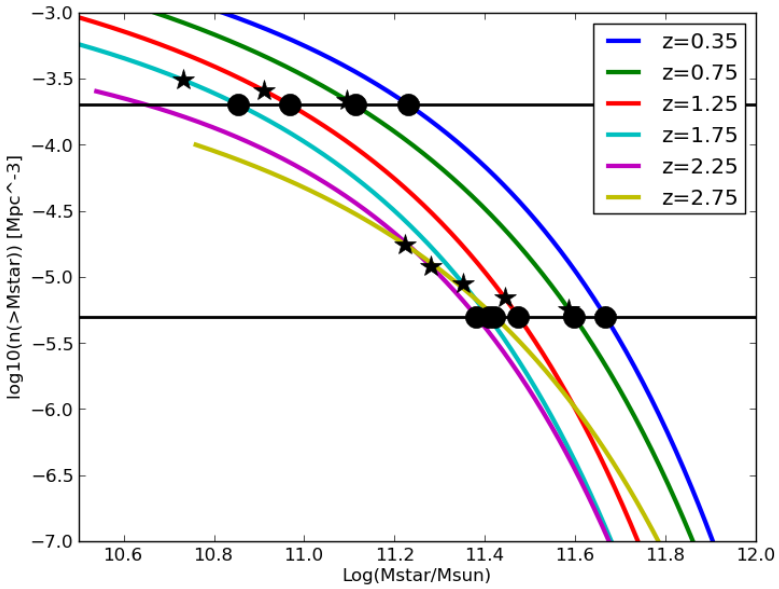


(a) Number Density vs Mass

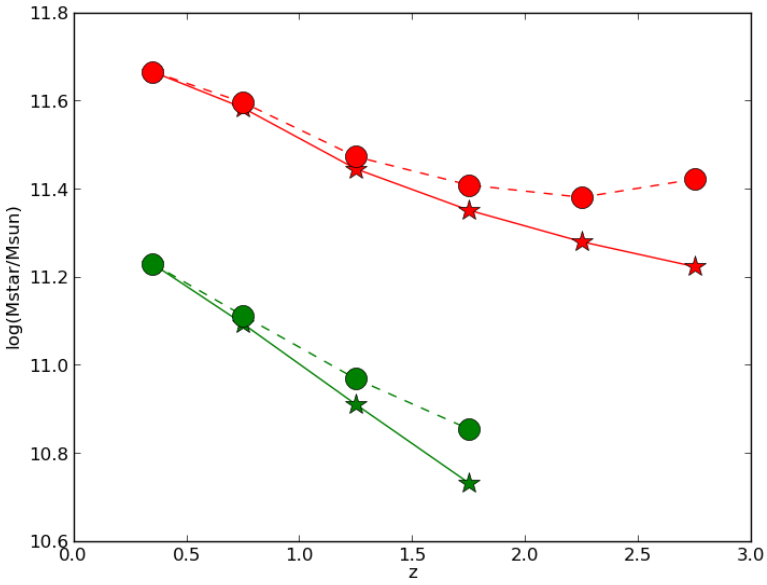


(b) Mass vs Redshift

Fig. I.5. The difference in mass evolution when merger history is accounted for. I.5(a): The differences between assuming constant number density (circles, no merging) and evolving number density (stars, accounts for merging of galaxies). The mass functions plotted in the background are taken from Muzzin et al. [2013]. I.5(b): Difference in mass evolution for two different starting masses as seen in I.5(a). Figure adapted from Behroozi et al. [2013].

# CHAPTER II

# DATA

## FAST parameters and data reduction

The primary driver in our analysis of LRGs is the mass evolution of the galaxy sample. To determine the distribution of masses from Redmapper, we use FAST to generate the stellar masses of our input catalog, which are shown in Fig. II.1. For FAST parameters, we fix the redshift to the photometric redshift provided by the Redmapper catalog, assume solar metallicity, a Chabrier [Chabrier, 2003] IMF, a delayed exponentially declining SFH, and a Calzetti dust law [Calzetti et al., 2000]. We also plot the expected progenitor masses for $z = 0.1$ LRGs with masses $10^{10} M_{\odot}$, $10^{10.5} M_{\odot}$, $10^{11} M_{\odot}$ ($M_{\odot}$ indicates units of solar mass).

To generate the mass of the progenitor galaxies from the number density predictions of Behroozi et al. [2013], we first determine (using the mass function of Bell et al. [2003]) the number density at $z = 0.1$ that corresponds to $10^{10} M_{\odot}$, $10^{10.5} M_{\odot}$, or $10^{11} M_{\odot}$. We then use this number density as an input to the number density calculator, and calculate the number density at some higher redshift $z'$. If this higher redshift $z'$ does not correspond to one of the redshifts for which an analytic mass function is available from Muzzin et al. [2013], we interpolate between analytic solutions using a quadratic function to determine the stellar mass of the progenitor at $z'$.

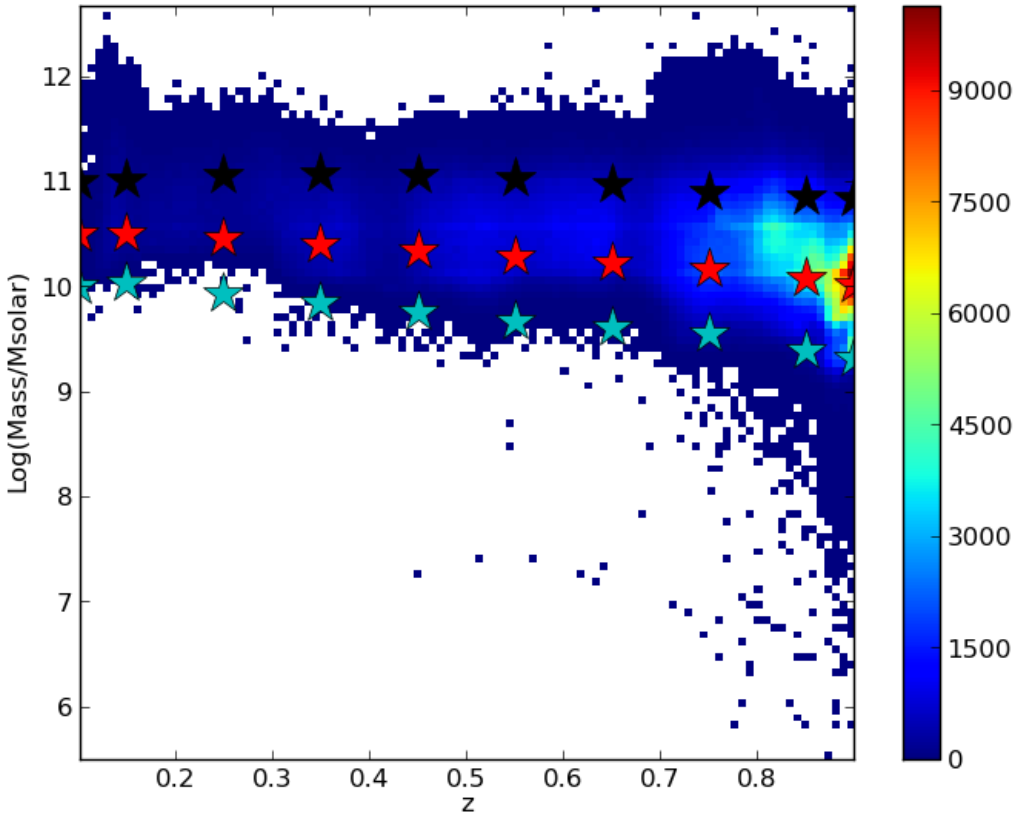


Fig. II.1. Mass evolution of LRGs from the Redmapper catalog. Overplotted as (cyan, red, black) stars are the expected progenitor masses of a $z = 0.1$ LRG with mass $10^{10} M_{\odot}$, $10^{10.5} M_{\odot}$, and $10^{11} M_{\odot}$

For the color evolution diagrams shown in Figures II.2, II.3, and II.4, we use the colors and redshifts of potential progenitors (marked by colored stars in figure II.1). Possible progenitors for color evolution are found by selecting all galaxies within a box centered on a progenitor of width 0.01 in redshift and a height of 0.2 dex in mass. The colors are then compared with models constructed via EzGal. As model parameters for EzGal, we use a Conroy stellar population model [Conroy et al., 2009, Conroy and Gunn, 2010] generated with a Simple Stellar Population (SSP) star formation history, with metallicities of both solar (z=0.019) and 0.5 times solar (z=0.0096). The SSPs fit the general shape of the LRG population well in the $r - i$ and $i - z$ colors, but are slightly offset in the $g - r$ color.

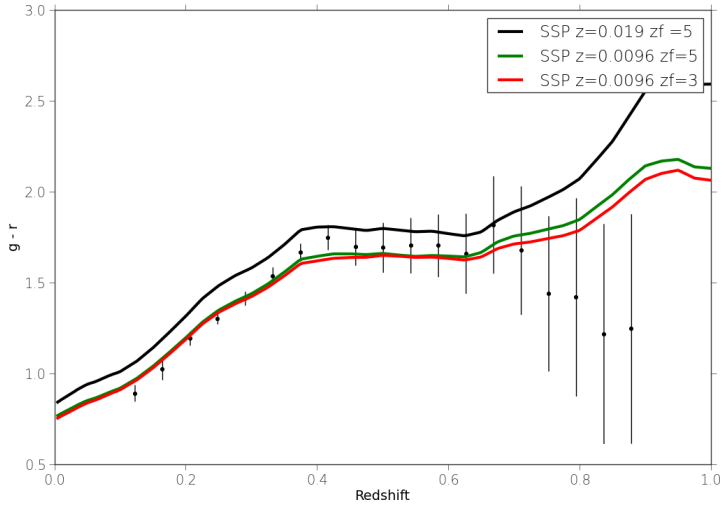


(a) $10^{10.5} M_{\odot}$

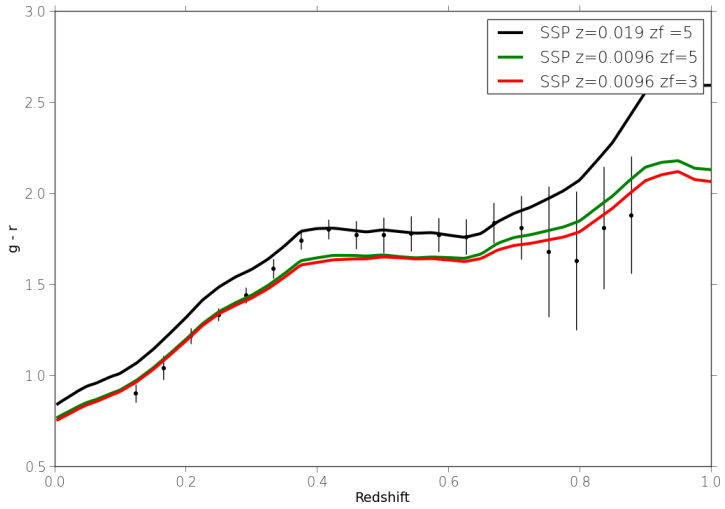


(b) $10^{11} M_{\odot}$

Fig. II.2. DES *g-r* Color evolution of the Redmapper galaxies. Upper row: color evolution of progenitors for $10^{10.5} M_{\odot}$ galaxies. Bottom row: color evolution of progenitors for $10^{11} M_{\odot}$ galaxies. The colors at each redshift are plotted as the median of the binned colors of potential progenitors selected as described in the text. Errors are plotted as the standard deviation of the binned colors. Plotted underneath are the expected color evolution models as calculated by the modeling code EzGal. EzGal models are generated as Simple Stellar Populations (SSP's) with both solar metallicity (z=0.019) and 0.5 solar metallicity (z = 0.0096). Models are generated with a formation redshift of either 3 or 5 (zf = 3,5). The observed color evolution is most consistent with a SSP with a metallicity of z = 0.0096 and a formation redshift of either 3 or 5, (12.5 and 11.5 Gyr old, respectively).

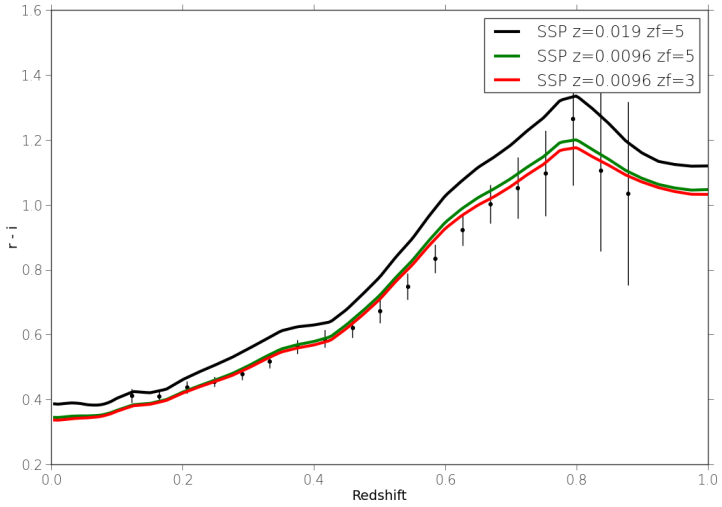


(a) $10^{10.5} M_{\odot}$

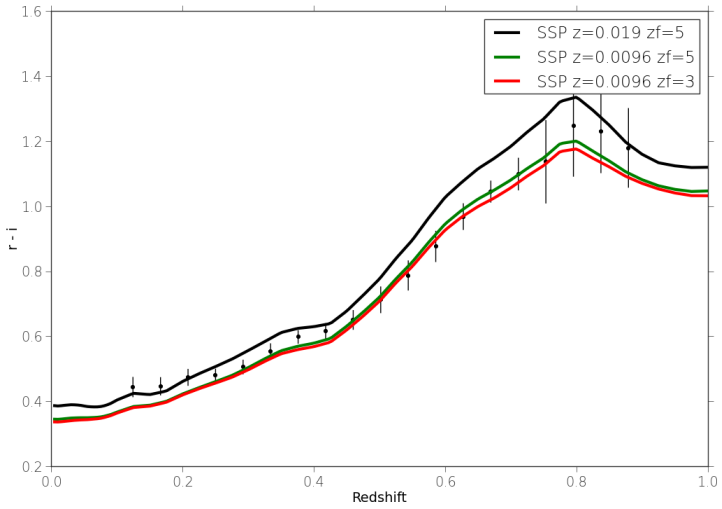


(b) $10^{11} M_{\odot}$

Fig. II.3. DES *r-i* Color evolution of the Redmapper galaxies. See Figure II.2 for details.

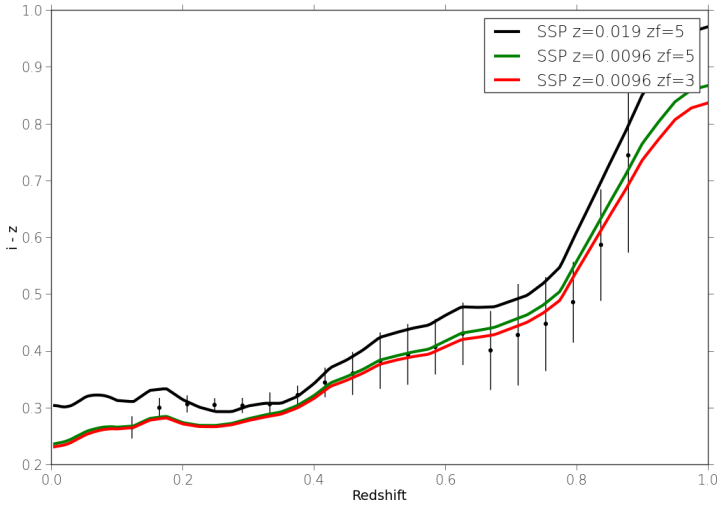


(a) $10^{10.5} M_{\odot}$

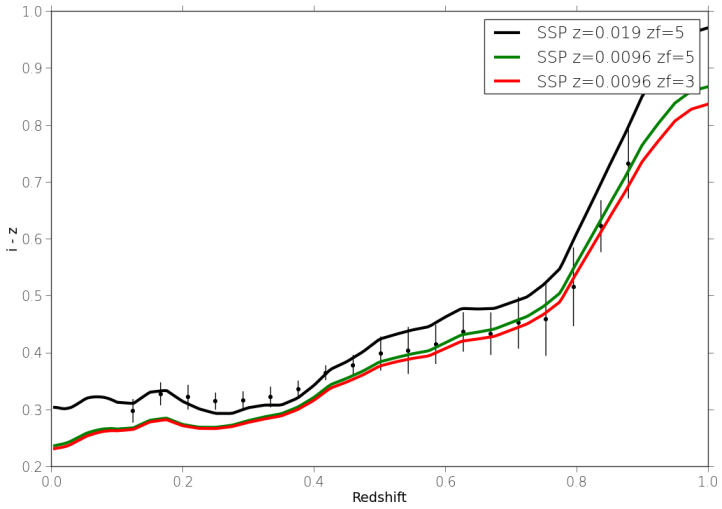


(b) $10^{11} M_{\odot}$

Fig. II.4. DES *i-z* Color evolution of the Redmapper galaxies. See Figure II.2 for details.

The color-color evolution of the population is shown in figures II.5 and II.6. The EzGal models are again overplotted with the parameters mentioned previously. Again, we see a good match in the $riz$ color-color diagram for the model evolution and observed colors, but small issues remain in the $gri$ color-color diagram, due to the mismatch in $g - r$.

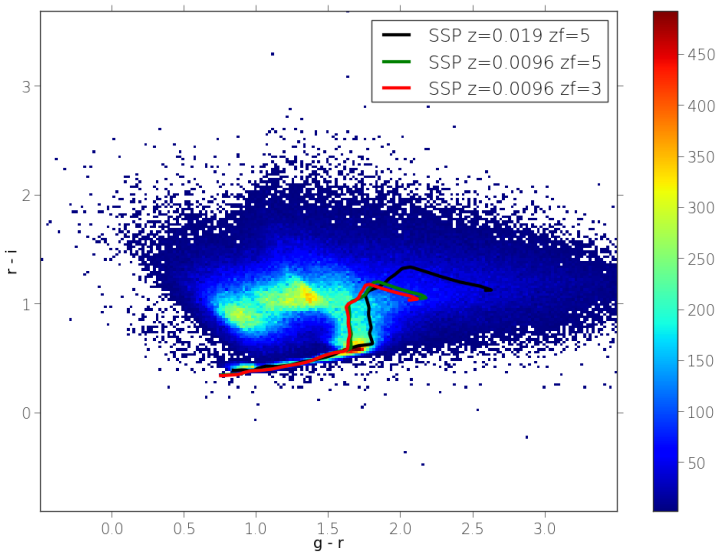


(a) $10^{10.5} M_{\odot}$

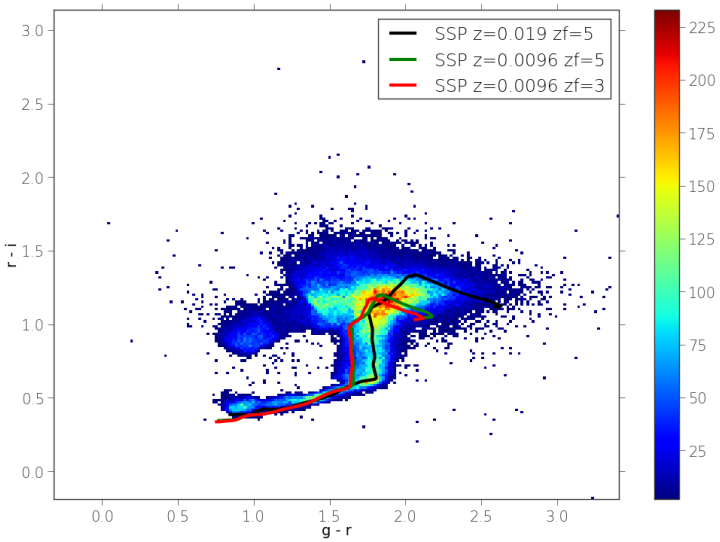


(b) $10^{11} M_{\odot}$

Fig. II.5. DES *gri* Color-color evolution of the $10^{10.5} M_{\odot}$ and $10^{11} M_{\odot}$ progenitors. Overplotted are the expected color-color evolution models as calculated by the modeling code EzGal(cite). EzGal models are generated as Simple Stellar Populations (SSP's) with both solar metallicity (z=0.019) and 0.4 solar metallicity (z = 0.0096). Models are generated with a formation redshift of either 3 or 5 (zf = 3,5). The observed color evolution is most consistent with a SSP with a metallicity of z = 0.0096 and a formation redshift of either 3 or 5, (12.5 and 11.5 Gyr old, respectively).

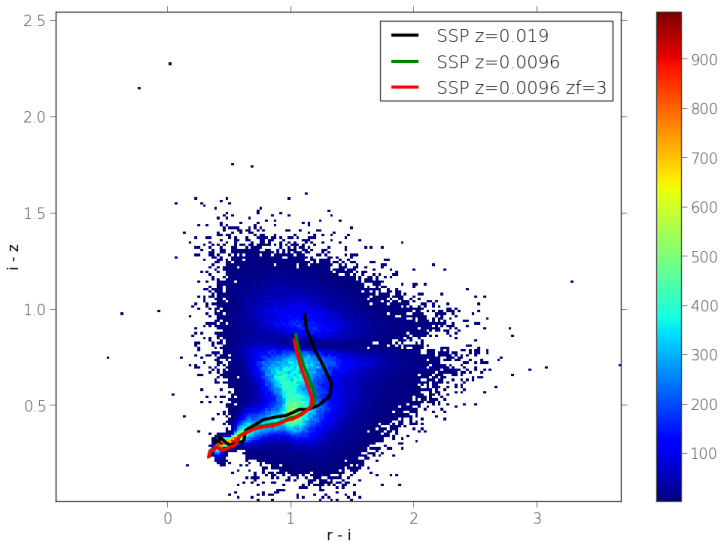


(a) $10^{10.5} M_{\odot}$

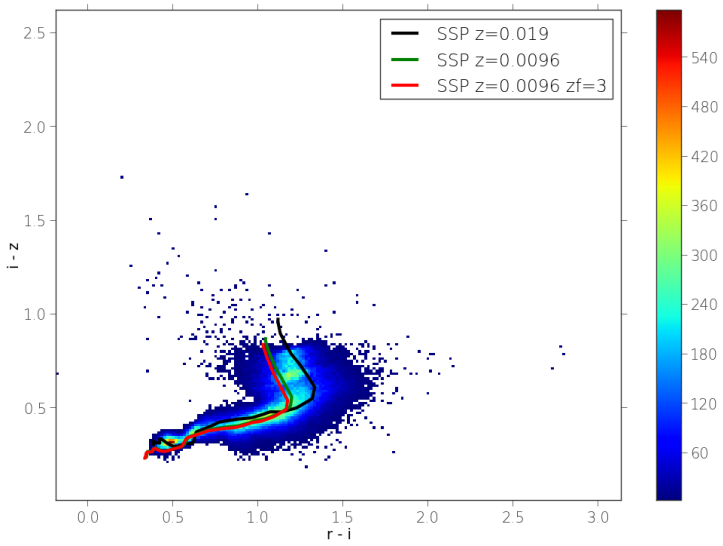


(b) $10^{11} M_{\odot}$

Fig. II.6. DES *riz* Color-color evolution of the $10^{10.5} M_{\odot}$ and $10^{11} M_{\odot}$ progenitors. See figure II.5 for details.

# CHAPTER III

# DISCUSSION

## Mass evolution

Figure II.1 indicates that most LRGs measured by the DES lie between $10^{10} M_{\odot}$ and $10^{12} M_{\odot}$. The overdensity of galaxies with a redshift of $z = 0.9$ is likely due to limitations in the photometry of the DES data. Since apparent brightness decreases with distance, these objects are typically the faintest in the catalog, and therefore have the poorest signal-to-noise ratio. This in turn decreases the ability of FAST to accurately recover masses.

Another factor affecting our ability to accurately measure progenitor masses (and color evolution) is known as progenitor bias [van Dokkum and Franx, 2001]. Progenitor bias is caused by the dropout of blue, starforming galaxies at high redshift from the pool of potential progenitors as selected observationally. Since LRGs are selected by essentially performing color cuts, blue galaxies at high redshift that may evolve into red, passive galaxies by $z = 0.1$ are neglected. This means that any pool of progenitors at a higher redshift will be redder than the actual pool of progenitors, so long as this effect is not taken into account. With only photometric data however, it is difficult to obtain accurate redshifts for these blue galaxies. It is also difficult to predict exactly which of the blue galaxies will quench star formation and evolve into a LRG.

## Color evolution

Figures III.1, III.2, and III.3 demonstrate clearly the color differences of the progenitors of $10^{10.5} M_{\odot}$ and $10^{11} M_{\odot}$ galaxies. On average, $10^{11} M_{\odot}$ galaxy progenitors are redder than their $10^{10.5} M_{\odot}$ pro-

genitor counterparts. One potential explanation for this is that more massive galaxies quench faster than their lower mass counterparts. Since the progenitors of $10^{11} M_{\odot}$ galaxies are predicted to be more massive than $10^{10.5} M_{\odot}$ progenitors, it is reasonable to expect that they are redder as well.

Progenitor bias could also play a role in relative blueness of the $10^{10.5} M_{\odot}$ progenitors, especially at low redshift. Since star forming galaxies tend to be less massive than their ETG counterparts, it could be that more star forming galaxies have evolved into $10^{10.5} M_{\odot}$ galaxies recently than $10^{11} M_{\odot}$ galaxies, leaving the colors of the $10^{10.5} M_{\odot}$ galaxies bluer in comparison.

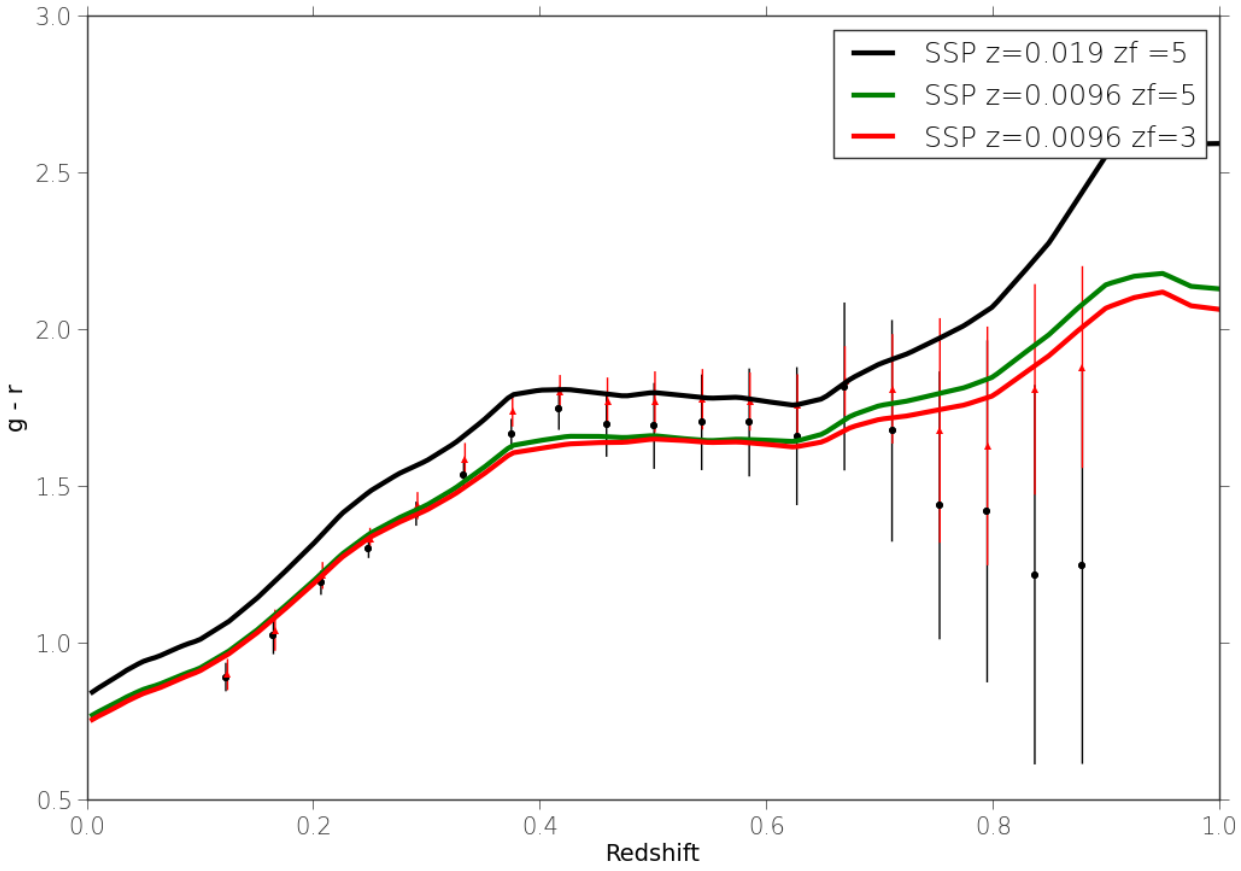


Fig. III.1. DES *g-r* Color evolution of the Redmapper galaxies, with both $10^{10.5} M_{\odot}$ (black circles) and $10^{11} M_{\odot}$ (red triangles) progenitors plotted. See Figure II.2 for details.

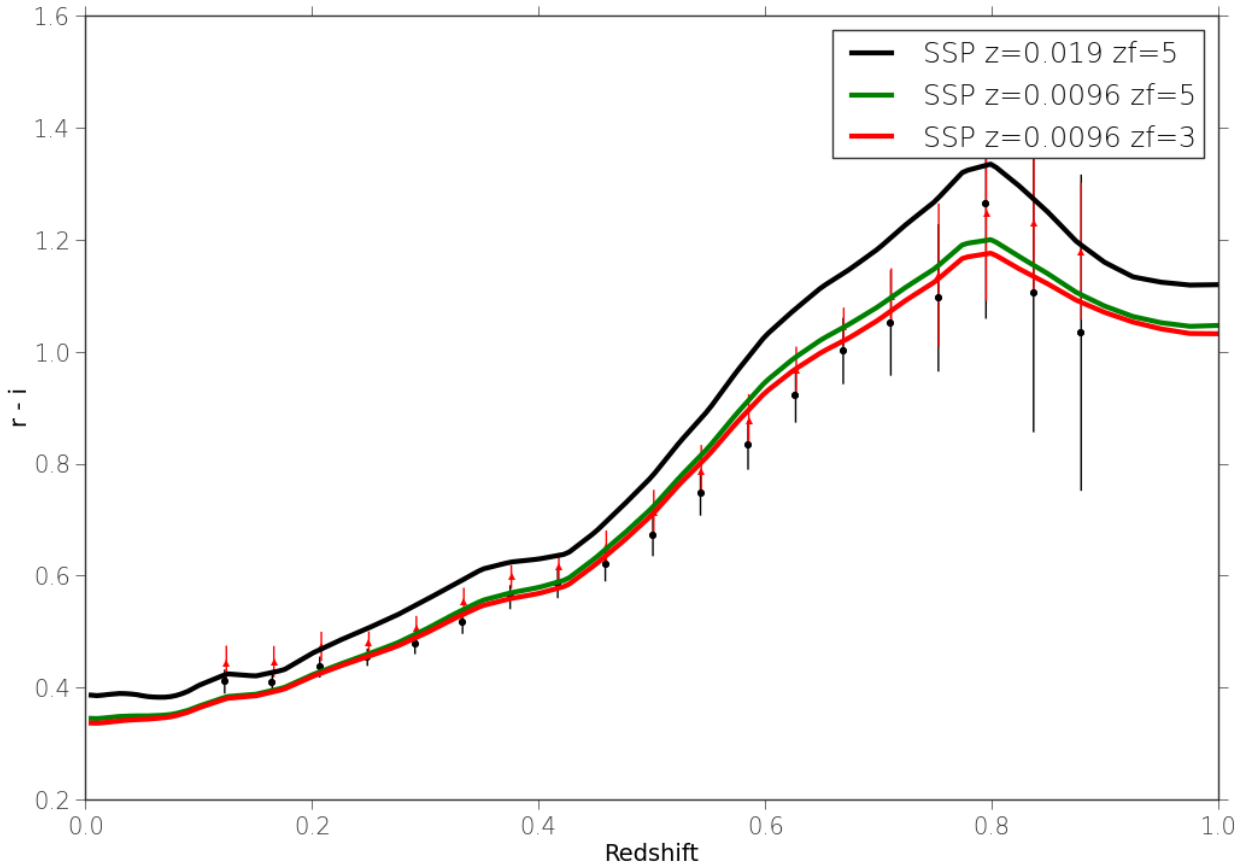


Fig. III.2. DES *r-i* Color evolution of the Redmapper galaxies, with both $10^{10.5} M_{\odot}$ (black circles) and $10^{11} M_{\odot}$ (red triangles) progenitors plotted. See Figure II.2 for details.

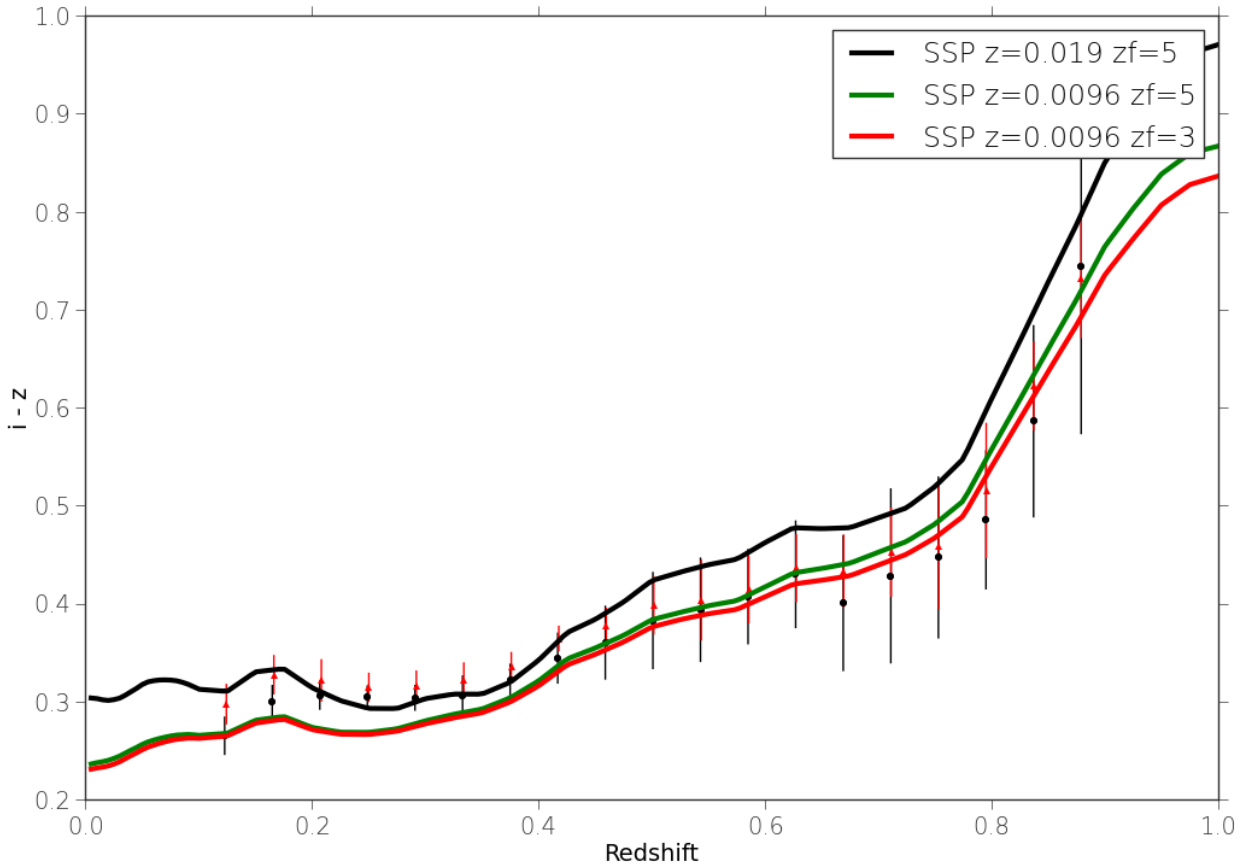


Fig. III.3. DES *i*-*z* Color evolution of the Redmapper galaxies, with both $10^{10.5} M_{\odot}$ (black circles) and $10^{11} M_{\odot}$ (red triangles) progenitors plotted. See Figure II.2 for details.

Progenitor bias does however provide a possible explanation for the blueness of the progenitors in the $g-r$ colors. Since these blue galaxies take time to redden once their star formation stops, LRGs descended from these recently star forming galaxies will appear bluer than their longer-quiescent brethren. This blueness however, is not observed in the $r-i$ or $i-z$ colors, so it may form only part of the explanation for the blueness at low redshift in $g-r$.

Another solution for the $g-r$ offset proposed by C. Conroy [private communication] is to change the models used. The models used here are systematically offset in $g-r$, so using alternate models could provide some additional relief in $g-r$ in particular. Another possible fix would be to use a non-SSP model for color evolution. Using a delayed exponential (e.g., of form $t\,e^{-\frac{t}{\tau}}$) would allow star formation to continue on for a short time after the galaxies are born, providing a small shift in the colors of the galaxies towards the blue. Resolving the $g-r$ color problem would likely also fix the offset in the $gri$ color-color diagram. Since the $g-r$ color plotted against any other color would always be offset, the color-color diagrams offer only a small amount of validation that the models provide reasonable estimates of the colors of LRGS.

**Future work**

There is much potential for future work using this LRG dataset. One possible avenue would be to explore the full systematics of different assumptions of e.g. metallicity in FAST, and their effects on the color evolution of progenitors.

Another possibility for future work is in expanding the pool of potential progenitors to reduce progenitor bias. By acquiring redshifts and masses for all galaxies, star forming or not, we can include blue, massive galaxies at high redshift in our progenitor estimates and evaluate their overall effect on model matching at high redshift. Since the Behroozi et al. [2013] number density modeling is

purely dark matter based, our mass predictions for progenitors ought to remain the same, so at a given redshift, the measured progenitor color should become bluer.

# REFERENCES


P. S. Behroozi, D. Marchesini, R. H. Wechsler, A. Muzzin, C. Papovich, and M. Stefanon. Using Cumulative Number Densities to Compare Galaxies across Cosmic Time. *ApJL*, 777:L10, November 2013. doi: 10.1088/2041-8205/777/1/L10.

E. F. Bell, D. H. McIntosh, N. Katz, and M. D. Weinberg. The Optical and Near-Infrared Properties of Galaxies. I. Luminosity and Stellar Mass Functions. *ApJS*, 149:289–312, December 2003. doi: 10.1086/378847.

G. Bruzual and S. Charlot. Stellar population synthesis at the resolution of 2003. *MNRAS*, 344: 1000, October 2003. doi: 10.1046/j.1365-8711.2003.06897.x.

D. Calzetti, L. Armus, R. C. Bohlin, A. L. Kinney, J. Koornneef, and T. Storchi-Bergmann. The Dust Content and Opacity of Actively Star-forming Galaxies. *ApJ*, 533:682–695, April 2000. doi: 10.1086/308692.

G. Chabrier. Galactic Stellar and Substellar Initial Mass Function. *Publ. Astron. Soc. Pac.*, 115: 763–795, July 2003. doi: 10.1086/376392.

C. Conroy and J. E. Gunn. The Propagation of Uncertainties in Stellar Population Synthesis Modeling. III. Model Calibration, Comparison, and Evaluation. *ApJ*, 712:833–857, April 2010. doi: 10.1088/0004-637X/712/2/833.

C. Conroy, J. E. Gunn, and M. White. The Propagation of Uncertainties in Stellar Population Synthesis Modeling. I. The Relevance of Uncertain Aspects of Stellar Evolution and the Initial Mass Function to the Derived Physical Properties of Galaxies. *ApJ*, 699:486–506, July 2009. doi: 10.1088/0004-637X/699/1/486.

O. J. Eggen, D. Lynden-Bell, and A. R. Sandage. Evidence from the motions of old stars that the galaxy collapsed. *ApJ*, 136:748, 1962.

M. D. Gladders and H. K. C. Yee. A New Method For Galaxy Cluster Detection. I. The Algorithm. *AJ*, 120:2148–2162, October 2000. doi: 10.1086/301557.

Mariska Kriek, Pieter G. van Dokkum, Ivo Labbé, Marijn Franx, Garth D. Illingworth, Danilo Marchesini, and Ryan F. Quadri. An ultra-deep near infrared spectrum of a compact quiescent galaxy at z=2.2. *ApJ*, 700:221, 2009.

K. Krisciunas. Optical Night-Sky Brightness at Mauna Kea over the Course of a Complete Sunspot Cycle. *Publ. Astron. Soc. Pac.*, 109:1181–1188, October 1997. doi: 10.1086/133993.

A. Muzzin, D. Marchesini, M. Stefanon, M. Franx, H. J. McCracken, B. Milvang-Jensen, J. S. Dunlop, J. P. U. Fynbo, G. Brammer, I. Labbé, and P. G. van Dokkum. The Evolution of the Stellar Mass Functions of Star-forming and Quiescent Galaxies to z = 4 from the COSMOS/UltraVISTA Survey. *ApJ*, 777:18, November 2013. doi: 10.1088/0004-637X/777/1/18.

M. Postman and T. R. Lauer. Brightest cluster galaxies as standard candles. *ApJ*, 440:28–47, February 1995.

E. S. Rykoff, E. Rozo, M. T. Busha, C. E. Cunha, A. Finoguenov, A. Evrard, J. Hao, B. P. Koester, A. Leauthaud, B. Nord, M. Pierre, R. Reddick, T. Sadibekova, E. S. Sheldon, and R. H. Wechsler. redMaPPer. I. Algorithm and SDSS DR8 Catalog. *ApJ*, 785:104, April 2014. doi: 10.1088/0004-637X/785/2/104.

L. Searle and R. Zinn. Compositions of halo clusters and the formation of the galactic halo. *ApJ*, 225:357, 1978.

The Dark Energy Survey Collaboration. The Dark Energy Survey. *ArXiv Astrophysics e-prints*, October 2005.

S. Toft, P. van Dokkum, M. Franx, I. Labbé, N. M. Förster Schreiber, S. Wuyts, T. Webb, G. Rudnick, A. Zirm, M. Kriek, P. van der Werf, J. P. Blakeslee, G. Illingworth, H.-W. Rix, C. Papovich, and A. Moorwood. Hubble space telescope and spitzer imaging of red and blue galaxies at z ˜ 2.5: A correlation between size and star formation activity from compact quiescent galaxies to extended star-forming galaxies. *ApJ*, 671:285, December 2007. doi: 10.1086/521810.

P. G. van Dokkum and M. Franx. Morphological Evolution and the Ages of Early-Type Galaxies in Clusters. *ApJ*, 553:90–102, May 2001. doi: 10.1086/320645.

Pieter G. van Dokkum, Katherine E. Whitaker, Gabriel Brammer, Marijn Franx, Mariska Kriek, Ivo Labb, Danilo Marchesini, Ryan Quadri, Rachel Bezanson, Garth D. Illingworth, Adam Muzzin,

Gregory Rudnick, Tomer Tal, and David Wake. The growth of massive galaxies since z = 2. *ApJ*, 709(2):1018, 2010. URL http://stacks.iop.org/0004-637X/709/i=2/a=1018.